Taylor & Francis
Taylor & Francis Group

Expert Opinion on Drug Delivery

ISSN: (Print) (Online) Journal homepage: www.tandfonline.com/journals/iedd20

3D printed personalized therapies for pediatric patients affected by adrenal insufficiency

Lucía Rodríguez-Pombo, Concepción Gallego-Fernández, Anna Kirstine Jørgensen, Carlos Javier Parramon-Teixidó, Carme Cañete-Ramirez, Maria Josep Cabañas-Poy, Abdul W. Basit, Carmen Alvarez-Lorenzo & Alvaro Goyanes

To cite this article: Lucía Rodríguez-Pombo, Concepción Gallego-Fernández, Anna Kirstine Jørgensen, Carlos Javier Parramon-Teixidó, Carme Cañete-Ramirez, Maria Josep Cabañas-Poy, Abdul W. Basit, Carmen Alvarez-Lorenzo & Alvaro Goyanes (18 Sep 2024): 3D printed personalized therapies for pediatric patients affected by adrenal insufficiency, Expert Opinion on Drug Delivery, DOI: 10.1080/17425247.2024.2399706

To link to this article: https://doi.org/10.1080/17425247.2024.2399706

Published online: 18 Sep 2024.

EXPERT OPINION ON DRUG DELIVERY
https://doi.org/10.1080/17425247.2024.2399706

Taylor & Francis
Taylor & Francis Group

ORIGINAL RESEARCH

OPEN ACCESS Check for updates

3D printed personalized therapies for pediatric patients affected by adrenal insufficiency

Lucía Rodríguez-Pombo[a], Concepción Gallego-Fernández[a], Anna Kirstine Jørgensen[b], Carlos Javier Parramon-Teixidó [c], Carme Cañete-Ramirez[c], Maria Josep Cabañas-Poy[c], Abdul W. Basit[b,d,e], Carmen Alvarez-Lorenzo [a] and Alvaro Goyanes[a,b,d,e]

[a]Departamento de Farmacología, Farmacia y Tecnología Farmacéutica, I+D Farma (GI-1645), Facultad de Farmacia, Instituto de Materiales (iMATUS) and Health Research Institute of Santiago de Compostela (IDIS), Universidade de Santiago de Compostela, Santiago de Compostela, Spain; [b]Department of Pharmaceutics, UCL School of Pharmacy, University College London, London, UK; [c]Pharmacy Department, Vall d'Hebron Hospital Universitari, Vall d'Hebron Barcelona Hospital Campus, Barcelona, Spain; [d]FABRX Ltd., Henwood House, Henwood, Ashford, Kent, UK; [e]FABRX Artificial Intelligence, Carretera de Escairón, 14, Currelos (O Saviñao), Spain

ABSTRACT

Background: Adrenal insufficiency is usually diagnosed in children who will need lifelong hydrocortisone therapy. However, medicines for pediatrics, in terms of dosage and acceptability, are currently unavailable.

Research design and methods: Semi-solid extrusion (SSE) 3D printing (3DP) was utilized for manufacturing of personalized and chewable hydrocortisone formulations (printlets) for an upcoming clinical study in children at Vall d'Hebron University Hospital in Barcelona, Spain. The 3DP process was validated using a specific software for dynamic dose modulation.

Results: The printlets contained doses ranging from 1 to 6 mg hydrocortisone in three different flavor and color combinations to aid adherence among the pediatric patients. The pharma-ink (mixture of drugs and excipients) was assessed for its rheological behavior to ensure reproducibility of printlets through repeated printing cycles. The printlets showed immediate hydrocortisone release and were stable for 1 month of storage, adequate for prescribing instructions during the clinical trial.

Conclusions: The results confirm the suitability and safety of the developed printlets for use in the clinical trial. The required technical information from The Spanish Medicines Agency for this clinical trial application was compiled to serve as guidelines for healthcare professionals seeking to apply for and conduct clinical trials on 3DP oral dosage forms.

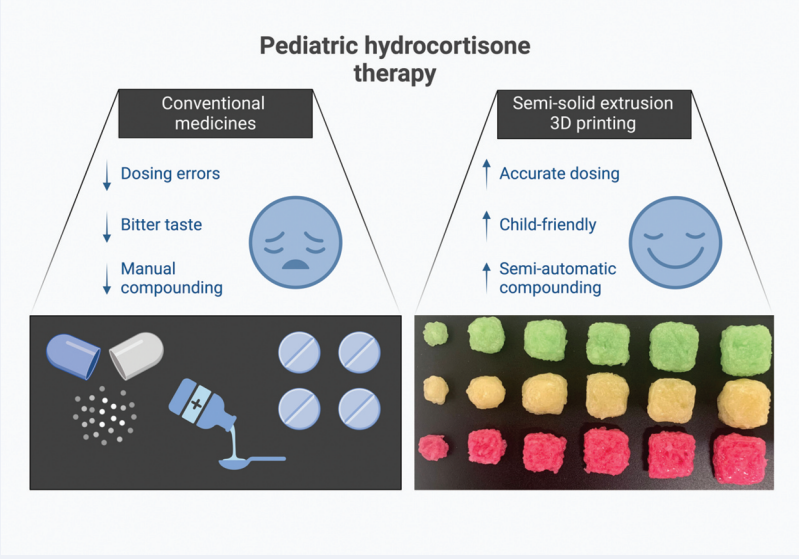

Created with BioRender.com

ARTICLE HISTORY

Received 4 June 2024
Accepted 23 August 2024

KEYWORDS

Direct ink writing 3D printing; patient acceptability of pharmaceuticals; oral drug products for paediatrics; personalised pharma-inks; additive manufacturing of medicines; chewable drug delivery systems; 3D printed medications; hydrocortisone formulations for children

CONTACT Alvaro Goyanes a.goyanes@fabrx.co.uk; Carmen Alvarez-Lorenzo carmen.alvarez.lorenzo@usc.es Departamento de Farmacología, Farmacia y Tecnología Farmacéutica, I+D Farma (GI-1645), Facultad de Farmacia,Instituto de Materiales (iMATUS) and Health Research Institute of Santiago de Compostela (IDIS), Universidade de Santiago de Compostela, 15782 Santiago de Compostela, Spain; Abdul W. Basit a.basit@ucl.ac.uk Department of Pharmaceutics, UCL School of Pharmacy, University College London, 29-39 Brunswick Square, London WC1N 1AX, UK

1. Introduction

Adrenal insufficiency is characterized by low cortisol blood levels due to absolute or partial cortisol production deficiency [1–3]. Three types of adrenal insufficiency exist: primary adrenal insufficiency (PAI), secondary adrenal insufficiency (SAI), and tertiary adrenal insufficiency (TAI). Congenital PAI and SAI are most frequently diagnosed in children and require lifelong therapy while TAI often presents as a consequence of exogenous glucocorticoid usage [4]. Therapy is based on cortisol replacement to closely resemble unimpaired physiological cortisol secretion patterns to avoid decompensations such as adrenal crisis and metabolic and cardiovascular disorders [5,6]. Cortisol secretion normally follows a circadian rhythm, with levels peaking in the morning and decreasing throughout the day to a minimum at night.

Hydrocortisone is the standard glucocorticoid for treating PAI and SAI in children and throughout puberty [7]. The recommended dose is 8–15 mg/m^2/day for administration two to three times daily, leading to variations in the required dose throughout the patient's life based on age, height, and weight [8,9]. The currently approved hydrocortisone medicines by the European Medicines Agency (EMA) include modified release tablet Plenadren® for adults [10] and modified release capsule Efmody® for adults and adolescents above the age of 12 years [11]. Recently, Alkindi®, immediate release hydrocortisone capsule, has been approved for pediatric usage, although side effects from discontinuation of conventional hydrocortisone therapy have led to limited availability in some countries [12].

Due to the lack of appropriate pediatric hydrocortisone medicines, the formulations are often prepared in hospitals as pharmaceutical compounding [13]. Utilized compounding techniques include crushing of marketed tablets for administration with foods, capsules filled with hydrocortisone granules, or preparation of suspensions [13–15]. However, pharmaceutical compounding is both heavily time-consuming and susceptible to human error [16]. A study reported that 21.4% of batches from pharmaceutical compounding of hydrocortisone showed inconsistencies in uniformity of mass or drug content while 3.6% did not comply with European Pharmacopoeia (Ph. Eur.) acceptance limits for labeled drug content [17]. This may lead to underdosing or exceeding of the recommended dose, which can result in loss of height at full development and other severe adverse effects [18,19]. Moreover, hydrocortisone is a drug with bitter taste, potentially compromising adherence to the compounded medicines and further reducing clinical outcomes among pediatrics.

In recent years, three-dimensional printing (3DP) technologies have emerged as alternatives to produce small batch and personalized drug products [20–23]. Highlighted as one of the more clinically advanced 3DP technologies, semi-solid extrusion (SSE) has the potential to prepare child-friendly medicines of precise doses with enhanced palatability and acceptability profiles [24–27]. SSE can deposit gels, waxes, or pastes to create solid or semi-solid objects, and it has facilitated the development of tailored 3DP drug delivery systems such as immediate or extended release printlets (3DP tablets) [28,29], chewable printlets [30,31], orodispersible films [32,33], polypills (multidrug-loaded printlets) [34,35], suppositories [36] and inserts [37].

Chewable printlets manufactured via SSE have previously been evaluated clinically in children affected by rare metabolic diseases [38,39]. The chewable printlets were equally as effective as the conventional medicines while demonstrating enhanced acceptability among the children in both studies. Additionally, bioequivalence of SSE printlets containing sildenafil citrate has been demonstrated in healthy adults [40], while SSE printlets manufactured in a hospital containing levothyroxine sodium were proven to be bioequivalent to tablet division and with enhanced disease management for infants affected by transient hypothyroxinaemia [41]. Although the published clinical data on SSE medicine manufacturing are promising, more clinical studies are needed to assess the technology's safety and efficacy across wider populations and pathologies. However, no regulatory frameworks or guidelines are currently applicable to developing and manufacturing printlets for clinical trials, potentially deterring efforts directed at this. Sharing of specific technical information requested by the different independent regulatory authorities may help to advance clinical implementation of 3DP medications further.

The aim of this work was to develop and validate an SSE 3DP process for the manufacture of personalized, chewable hydrocortisone medicines for technology transfer to Vall d'Hebron Hospital to conduct a clinical study (EudraCT number: 2021-001069-20 and NCT number: NCT06435481) in children aged 6–17 affected by PAI, SAI, or TAI. The chewable printlets were characterized in terms of physicochemical properties, chewability, drug content, *in vitro* release profile, and stability to ensure the quality of medicines and their appropriateness for inclusion in the clinical study. The personalized printlets contained doses ranging from 1 to 6 mg hydrocortisone, and the inclusion of three different colors and flavors in the pharma-ink (drug-loaded formulation for 3DP) altered the sensory characteristics of the printlets to be able to aid adherence among the children. An overview of the required technical information for the approval to conduct this clinical study by The Spanish Agency of Medicines and Medical Devices (AEMPS) has been compiled to serve as a guideline for the pharmaceutical 3DP community wishing to design and conduct further clinical studies on personalized 3DP medicines.

2. Materials and methods

2.1. Materials

High methyl-esterified (HM) pectin was obtained from Ceamsa (degree of esterification = 59.50%; pH = 3.20; O Porriño, Spain). Maltodextrin and maltitol were obtained from Roquette (Lestrem, France). Citric acid monohydrate, potassium citrate, yellow, green, and red colorants were purchased from Guinama (Valencia, Spain). Hydrocortisone base (MW 362.46 g/mol), strawberry, banana, and orange flavors were purchased from Acofarma (Barcelona, Spain). Methanol (HPLC grade) and potassium sodium tartrate tetrahydrate were obtained from Merck KGaA (Darmstadt, Germany), and formic acid (99–100% v/v) from VWR International (Radnor, USA). Hydrochloric acid (37%, Ph. Eur) was purchased from

Scharlau (Barcelona, Spain), potassium dihydrogen phosphate from ITW Reagents (Barcelona, Spain), and sodium phosphate tribasic dodecahydrate (≥98.0% w/w) from Honeywell Fluka (Buchs, Switzerland). All materials were used as received.

2.2. Preparation of hydrocortisone pharma-ink

The pharma-inks were prepared following a standard operating protocol. The composition of the pharma-inks is property of FABRX Ltd. (London, UK), but the excipients were sucrose, pectin, maltodextrin, water, maltitol, potassium citrate, potassium sodium tartrate tetrahydrate, flavorings, colorants, citric acid, and 0.4% w/w hydrocortisone. Pharma-inks based on different flavors and colors were developed according to Vall d'Hebron Hospital requirements and the protocol approved by the Spanish Agency of Medicines for the clinical trial (EudraCT: 2021-001069-20 and NCT: NCT06435481) in children with adrenal insufficiency. The flavor and color combinations were as follows: strawberry-red, orange-green, and banana-yellow.

Briefly, the solid excipients except maltitol were incorporated into water under magnetic stirring on a hot stirrer plate to prevent pectin lumps. After the dispersion in water, maltitol was added to the mixture under stirring, followed by heating the formulation to 80 °C for 10 min. After heating, the hot stirrer plate temperate was reduced to 65 °C. Then, hydrocortisone and the flavoring and coloring agents were added under stirring. Citric acid was added as a solution to gel the pectin. The resulting pharma-ink was transferred to 20 ml disposable, sterile luer lock syringes (B.Braun, Melsungen, Germany) and cooled at room temperature for 24 h. The syringes were kept protected from light to avoid any photodegradation [42,43].

2.3. Rheological properties of pharma-ink and pH values

Rheological characterization of the pharma-ink was performed, in triplicate, using an Anton Paar rheometer (MCR 302 model, Graz, Austria) equipped with a H-PTD200 Peltier hood and an aluminum plate (15 mm in diameter). The gap and the temperature were fixed at 1 mm and 50 °C, respectively. The syringe containing the pharma-ink was kept in an oven (Heraeus I42, Hanau, Germany) at 50 °C for 10 min to mimic the conditions before printing process. Samples of the pharma-ink were manually and directly extruded on the platform of the rheometer. The test consisted of five steps in amplitude sweep mode recording G′ (storage modulus) and G′′ (loss modulus) to evaluate the self-healing properties of the pharma-ink, as follows: 1) 0.5% shear strain for 300 s; 2) 100% shear strain for 100 s; 3) 0.5% shear strain for 300 s; 4) 100% shear strain for 100 s; and 5) 0.5% shear strain for 300 s. Data were recorded using the Anton Paar RheoCompass software (version 1.25, Anton Paar, Graz, Austria).

The pH measurement of the pharma-ink was carried out after dilution of 5 g of the pharma-ink in 95 ml of distilled water under magnetic stirring (300 rpm). The pH was measured in triplicate using a GLP 22 Crison pH meter (Crison Instruments, Barcelona, Spain).

2.4. Optimization and validation of SSE 3DP process of chewable printlets

Chewable printlets containing personalized hydrocortisone doses were manufactured using the pharmaceutical 3D printer M3DIMAKER™ (FABRX Ltd., London, UK) with the SSE printhead function. 16-Gauge tapered tips (Ellsworth Adhesives, Germantown, Wisconsin, USA) were used during the printing process.

Optimization and validation of the printing parameters of the pharma-ink was carried out with the M3DIMAKER Studio™ software wizard to establish correlations between the parameters and the sizes, weights, and doses of the printed objects. A rounded-corner cuboid ($10 \times 10 \times 4$ mm) model was selected from the software repository. The printing parameters were 20% infill density in rectilinear fill pattern, 1 mm layer height, two perimeters, 15 mm/s printing speed, 5 mm filament diameter, and 1.2 mm diameter nozzle (Ellsworth Adhesives, Germantown, USA). The printing temperature was 50 °C with the pharma-ink loaded syringe held at 50 °C for 10 min prior to extrusion.

A batch of 20 printlets were printed in four rows of five printlets each, with varying sizes and weights per row. The weight of each printlet was measured with an analytical balance (E42 model, Gibertini Elettronica, Novate Milanese, Italy), and the mean weight per row was calculated and inputted in the software for internal calibration and correlation of printing parameters, sizes, weights, and doses of the final printed objects. Calibrating the printer and software enabled the selection of target dose (i.e. 2 mg) as printing settings for the selected model from 1 mg up to 6 mg.

Different batches containing doses ranging from 1 to 6 mg were printed, as outlined in Table 1. The theoretical dose and the weight of the selected printlets, containing the lower and upper acceptance limits for mass uniformity according to the Ph. Eur [44], are also presented in Table 1.

The dimensions of each printlet were determined using a Vernier digital caliper (SIBUR International GmbH, Vienna, Austria), followed by weighing of each individual chewable printlet (Section 2.5) and transferring to Class B X-Large amber PVC blisters (Health Care Logistics, Circleville, USA).

2.5. Mass uniformity testing

A mass uniformity test was conducted immediately after the printing process by weighing each printlet individually ($n = 20$) using an analytical balance (E42 model, Gibertini Elettronica, Novate Milanese, Italy). Comparisons of the actual printlet weights to their declared theoretical weights (250, 500, 750,

Table 1. Theoretical dose and weight of the printlets. Limits of the mass range that is within the ±5% limits described in the Ph. Eur. For tablets of mass ≥250 mg.

Dose (mg)	Weight (mg)	Lower limit (mg)	Upper limit (mg)
1	250	237.2	262.5
2	500	475	525
3	750	712.5	787.5
4	1000	950	1050
5	1250	1187.5	1312.5
6	1500	1425	1575

1000, 1250, and 1500 mg) were carried out. According to the Ph. Eur. monograph for tablets with masses less than 250 mg, an individual mass deviation of 5% is accepted. Should a printlet deviate by more than 5%, it is removed and rejected from the batch. The acceptance limits for printlets of each dose are stated in Table 1.

2.6. Structural and physicochemical characterization of the printlets

2.6.1. X-ray powder diffraction (XRPD)

X-ray diffraction patterns of crystalline powder materials (hydrocortisone, pectin, sucrose, maltodextrin, potassium citrate, and potassium sodium tartrate tetrahydrate) were obtained with a D8 Advance diffractometer (Bruker, Billerica, MA, USA) using the Bragg-Brentano focusing geometry, equipped with a sealed X-ray tube (CuKα1 (λ = 1.5406 Å)) and a LYNXEYE-type detector. Samples were deposited on an oriented Se(511) plate which was rotated during measurement to obtain optimal peak profiles for analysis and to minimize the effect of the preferential orientation.

X-ray diffraction patterns of the pharma-ink and printlets were obtained in an Empyrean-type diffractometer (Malvern Panalytical, Malvern, UK), equipped with a five-axis goniometer (Chi-Phi-x-y-z platform). The X-rays were obtained from a sealed Cu tube of the Empyrean Cu LFFHR type (CuKα1 (λ = 1.5406 Å)). The detection of X-rays from the sample was carried out with a PANalytical PIXcel-3D type area detector. The incident radiation beam was focused with a multilayer parallel beam mirror, to work with rough, non-planar surfaces. The intensity and voltage applied were 40 mA and 40 kV, respectively. The diffractograms were obtained in the 2θ angular range of 3–50°, with a step of 0.04° and a counting time of 4 s per step.

2.6.2. Fourier transform infrared spectroscopy (FTIR)

The attenuated total reflectance FTIR (ATR-FTIR) spectra of the drug, excipients, and printlets were collected using a Varian 670 FTIR spectrometer (Varian Inc., Palo Alto, USA). All samples were scanned between 4000 and 400 cm^{-1} at a resolution of 4 cm^{-1} for 32 scans.

2.7. Hydrocortisone content in chewable printlets

The hydrocortisone contents of the printlets with different doses (1–6 mg) were determined. For 2–5 mg doses, a printlet was placed in a beaker with 50 ml Milli-Q water under magnetic stirring (300 rpm) overnight ($n = 10$). For the lowest (1 mg) and the highest (6 mg) doses, the contents of 10 printlets from three different batches ($n = 30$) were determined to assess the batch-to-batch variability, according to procedure for the other printlets. Kruskal–Wallis statistical test was performed to analyze if there were significant differences in terms of hydrocortisone content between the batches containing the same dose (batch-to-batch variability) ($p < 0.05$). All statistical analyses were performed using GraphPad Prism (v9.0.2, Dotmatics, Boston, USA).

Samples of the resulting solutions were filtered through 0.22 µm filters (Millipore Ltd., Dublin, Ireland) and the concentration of hydrocortisone determined with HPLC-UV system (JASCO LC-4000 Series, Jasco, Spain). The assay specified injecting 30 µL samples for analysis using a mobile phase, consisting of methanol (70% v/v) and water with 1% v/v formic acid (30% v/v), through a Symmetry 5 µm C18 column, 4.6 mm × 250 mm (Waters, Milford, MA, USA) maintained at 30 °C. The mobile phase was pumped at a flow rate of 0.6 ml/min, and the eluents were screened at a wavelength of 250 nm. The run time was 10 min, and the retention time for hydrocortisone was 7.2 min in the concentration range of 0.07–160 µg/ml.

2.8. Mechanical properties

Chewable printlets (14 mm side × 5 mm height) were evaluated, in duplicate, using a TA.XT Plus Texture Analyzer (Stable Micro Systems, Surrey, UK) equipped with a 30 kgf (~294 N) load cell. The samples were subjected to five successive stress –strain cycles (pre-assay and post-assay speeds were 1.0 mm/s) to simulate chewing, applying an uniaxial compression along their short axis (height) by downward movement (1.0 mm/s) of an aluminum cylinder probe (20 mm in diameter). The activation strength was set at 0.0010 N. In each cycle, the chewable printlet was compressed until a force of 100 N or 120 N was reached since the FDA recommends a hardness <118N for chewable tablets [45].

The force-displacement data were recorded for each compression cycle and later converted to engineered stress and strain, using the initial dimensions of the printlet. The Young's modulus was calculated as the slope of the initial linear region of the stress–strain curves to evaluate the deformation capacity of the printlet. The area under the stress–strain curve (AUC) was calculated in each of the five cycles. The chewing difficulty index (CDI) was also calculated as the following Equation 1:

$$CDI = F_h \cdot H \quad (1)$$

where F_h is the load or force needed to break the printlet (also known as hardness or breaking force, in newtons) and H is its height or thickness (in meters) [45].

2.9. In vitro *dissolution test*

The hydrocortisone release profiles from 1 to 6 mg printlets were obtained using an SR8-Plus Dissolution Test Station (Hanson Research, Chatsworth, CA, USA) with USP-II apparatus. The Dissolution Test Station was connected to a pump system named Auto Plus DissoScan (Hanson Research, Chatsworth, CA, USA). Four assays were carried out in different dissolution media according to Ph. Eur. and U.S. Pharmacopoeia (USP): 0.1 M HCl (pH = 1.2), phosphate buffer solution (pH = 4.5), phosphate buffer solution (pH = 6.8), and water, based on USP monograph corresponding to hydrocortisone tablets [46]. Sink conditions were maintained for all tests.

In each assay, the printlets were placed at the bottom of the vessel in 900 ml of dissolution media under constant paddle stirring (50 rpm) at 37 ± 0.5 °C. During the dissolution test, samples of hydrocortisone were automatically removed and filtered through 10 µm filters, and drug concentration was

determined using an in-line UV spectrophotometer (Agilent 8453 UV–Vis spectrophotometer, Agilent, Santa Clara, USA) operated at 250 nm. After each measurement, the samples were automatically returned to each dissolution vessel, keeping volume constant. At the end of the assay, samples of 5 ml of each vessel were withdrawn and filtered through 0.22 µm filters (Millipore Ltd., Dublin, Ireland), and the final amount of hydrocortisone released was analyzed using HPLC-UV method, as described in section 2.7. Data were reported throughout as mean ± standard deviation.

2.10. Hydrocortisone-loaded chewable printlets stability

Stability tests were carried out to investigate the stability of hydrocortisone within the chewable printlets under normal storage conditions (Class B X-Large amber PVC blisters). As the chewable printlets were intended for extemporaneous use, a shelf life of 1 month was predefined. According to the recommendations of the International Council for Harmonisation (ICH) guidelines for stability tests [47], the test was conducted on 10 printlets from three different batches containing the lowest dose (1 mg) and 10 printlets from three batches containing the highest dose (6 mg). Printlets were stored in Class B X-Large amber PVC blisters in a climatic chamber (CCSR 0150 model, Ineltec, Barcelona, Spain) for 1 month. The temperature and relative humidity conditions were 30 °C and 65%, according to ICH and WHO guidelines classifying Spain in climatic zone II [48]. Hydrocortisone content of each printlet was determined via HPLC-UV as described in section 2.7 after 1 month of storage. Acceptance limits for tablet content uniformity were used for evaluation of hydrocortisone content in the stability study [49].

Kruskal–Wallis statistical test was performed to analyze if there were significant differences in terms of hydrocortisone content between the batches containing the same dose (batch-to-batch variability) and between batches before 1 month storage ($p < 0.05$). All statistical analyses were performed using GraphPad Prism (v9.0.2, Dotmatics, Boston, USA).

2.11. Technical information on pharma-ink and printlets required by the Spanish agency of medicines and medical devices (AEMPS)

Regulatory agencies require extensive information to grant approval of clinical trials; however, there is no specific regulatory framework for 3D printing of medicines. Ensuring the quality of the dosage forms is crucial, involving quality control assays such as mass or content uniformity, drug release, impurity control, and stability of the active ingredient. These quality control tests are not always clearly defined, as is the case for chewable tablets, due to the lack of specific monographs in the European or U.S. Pharmacopeias [25].

The competent regulatory body, in this case, The Spanish Agency of Medicines and Medical Devices (AEMPS), required mandatory assays and requested additional information after the first application. The specific technical information that was provided to AEMPS for the manufacturing process and product quality is presented in Table 2.

Table 2. Technical information on the manufacturing process of pharma-ink and printlets and their quality provided to the AEMPS for approval to conduct the clinical study.

Topic	Specific documents, data, and information
A) Components and process	– Novelty of the formulation composition. Examples of similar formulations in other clinical studies – Similarity of the excipients and 3D printing process to other pharmaceutical processes – Candy-like aspect of the final pharmaceutical product
B) Reproducibility of the pharma-ink preparation	– Standard Operating Procedure for the preparation of the pharma-ink – Well-defined parameters (composition of the pharma-ink, pH, preparation temperature, stirring speed, mixing process, cooling process)
C) Reproducibility of the 3D printing process	– Validation of printing parameters (printing speed and extrusion temperature) – Software and hardware information
D) Mass uniformity assay	– Mass variation during the printing process in accordance with limits specified in Ph. Eur. monograph: 2.9.5. Uniformity of mass of single-dose preparations
E) Content uniformity assay	– HPLC stability indicating method – Absence of drug degradation and impurities – Ph. Eur. monograph: 2.9.6. Uniformity of content of single-dose preparations
F) Drug release profiles	– Drug dissolution test at different pH (1.2, 4.5, and 6.8) – Tests on intact chewable printlets (as recommended by FDA) – Comparison of profiles to conventional dosage form (if it is not a liquid) – Ph. Eur monographs: 2.9.3. Dissolution test for solid dosage forms 5.17.1. Recommendations on dissolution testing
G) Stability test	– ICH Guidelines for experimental design – No degradation products or impurities formed after 1 month storage – Data supported by literature
H) Microbiological control	– Microbiological control during the clinical trial – Total aerobic microbial count (TAMC) and total combined yeasts/molds count (TYMC) – Membrane filtration or plate-count methods to be used – Ph. Eur. monographs: 2.6.12. Microbiological examination of non-sterile products: microbial enumeration tests 2.6.13. Microbiological examination of non-sterile products: test for specified micro-organisms 5.1.4. Microbiological quality of non-sterile pharmaceutical preparations and substances for pharmaceutical use

3. Results and discussion

3.1. Pharma-ink development and characterization

The gelling agent, pectin, was added covering a range of contents from 0.5 to 3 g (corresponding to 0.27 g pectin per g citric acid solution and 1.64 g pectin per g citric acid solution, respectively) to investigate the optimal concentration for the pharma-ink in terms of printability and mechanical properties of the chewable printlets. Pharma-inks containing 0.5–2 g of pectin exhibited too weak semisolid characteristics, resulting in 3DP objects with unsatisfactory mechanical properties such as excessive stickiness and printlet collapse. An increase in required extrusion temperature was observed with the increase in pectin concentration due to the viscosity of the final gel. The pharma-ink containing 2.5 g of pectin displayed semisolid nature after cooling at room temperature for 24 h, good flow properties when printing at 50 °C (as explained below), as well as 3DP objects with appropriate mechanical properties. Employment of lower temperatures resulted in too viscous pharma-ink for extrusion while higher temperatures resulted in too liquid-like pharma-ink. The printed layers solidified rapidly during the printing process, creating a support structure for the following layers, preventing collapse of the printlet while ensuring appropriate handling properties of the printlets.

A portion of the optimized pharma-ink (containing 2.5 g of pectin) was extruded directly from the plate of the rheometer to characterize its rheological (self-healing) properties (Figure 1). The amplitude sweep tests were recorded under different strain conditions that mimic rest-like situations in the syringe (0.5% shear strain) and then maximum stress (100% shear strain) during the extrusion through the nozzle. A variety of rheological methods have been tested to characterize the properties of pharma-inks to obtain directly translatable information on the performance during 3D printing [50–55]. The conditions selected in the present study were shown representative previously [56] to obtain information about the recovery of the consistency once the pharma-ink was deposited on the printing platform and the feasibility of using the same pharma-ink for successive printing of several printlets.

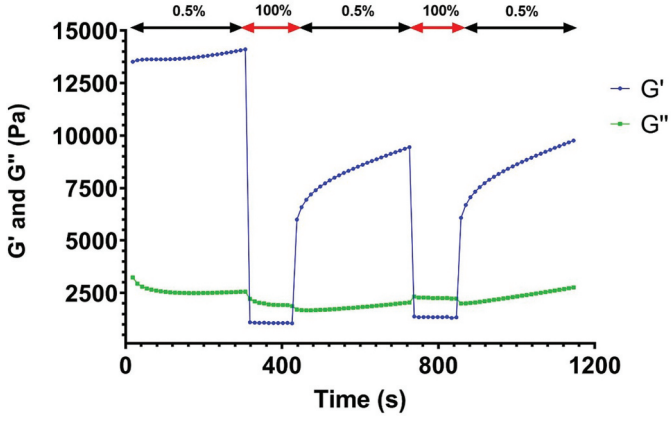

Figure 1. Storage modulus (G′) and loss modulus (G″) of the hydrocortisone pharma-ink. Black and red lines indicate the shear strain conditions of 0.5% and 100%, respectively.

The 3DP process involves several steps that require unique and complex rheological behaviors of the pharma-ink [24]. When pressure is applied on the syringe, the pharma-ink should be delivered through the nozzle at a constant flow to obtain a continuous deposition. On the other hand, the pharma-ink should not flow when the pressure is not applied or removed. Moreover, once deposited on the platform, the pharma-ink layer should exhibit a rapid recovery to support the following layers. This balance can be quantified using the loss factor or tan δ (=G″/G′). The loss modulus (G,″ viscous part) represents the flow properties of a material, and the storage modulus (G,′ elastic part) reflects the immediate recovery of a material. The ratio of the loss modulus to the storage modulus, defined as the damping factor or loss factor, indicates the relative energy of dissipation or damping of the material. This means that for a material with tan $\delta > 1$ the viscous part will have a greater influence on the final properties of the material. Under 0.5% shear strain, G′ values were higher than G″ values by 5–2.5 times (tan δ values between 0.20 and 0.40, depending on the shear strain cycle), resulting in elastic predominant behavior, whereas the opposite behavior was observed under 100% shear strain. This confirmed that the pharma-ink would not flow at lower shear strain values, conditions similar to those being stored in syringe and removal of pressure. On the other hand, it would start to flow at applied pressure during the 3DP process, ensuring continuous deposition of material in a layer-by-layer manner. Moreover, G′ rapidly recovers and exceeds G″ after the different sheer strain cycles, indicating that the pharma-ink was suitable for the 3DP process where strain is applied over multiple cycles to create multiple printlets. This resulted in deposited material on the printing platform with high consistency, ensuring the successful deposition of successive layers of the 3D printed object, avoiding collapse. This was further enhanced by the decrease in temperature from 50 °C (extrusion temperature) to room temperature as the material solidified faster due to the temperature-reversible behavior of pectin.

Pectin is a natural and linear polysaccharide consisting of D-galacturonic acid (GalA) units joined in chains by α-(1-4) glycosidic bonds [57], and pH plays an important role in the gelling mechanism of some pectin types. The pectin chains contain carboxylic acid groups due to galacturonic acid, and the chains are able to interact and assemble, leading to the formation of 3D networks in which water and solutes can be trapped [58]. Pectins are commonly classified based on the degree of esterification (DE) of carboxyl groups as high methyl-esterified (HM) or low methyl-esterified (LM) pectins [59] which play an important role in their functional properties. HM-pectins usually have a DE above 50% while LM-pectins have a DE less than 50% [60]. The chemical structure and gelling mechanism of pectin along with factors such as temperature, pH, presence of sugars and other solutes, and divalent cations play an important role in pectin gelation [61]. The hydrocortisone pharma-inks prepared in this study presented a pH of 3.99 ± 0.27.

HM-pectin with highly soluble solid contents, at least 55%, forms a gel in an acidic medium in the presence of abundant sugar [59,61]. The presence of H^+ decreases the dissociation of

free carboxyl groups, thus reducing electrostatic repulsion between molecular chains [59]. On the other hand, abundant sugar contributes to reduction of the hydrated radius of pectin and, therefore, results in inter-chain interactions rather than chain-water molecule interactions [61,62]. In addition, the hydrophobicity of the methyl groups could also promote the inter-chain interaction [58]. Therefore, the junction zones are formed by the cross-linking of homogalacturonan by hydrogen bridges and hydrophobic forces between methoxyl groups, both promoted by high sugar concentration and acidic pH.

Conversely, LM-pectins gel is independent of sugar content, and they are not as sensitive to pH as the HM-pectins [60]. LM-pectins require the presence of divalent cations for gelation. Junction zones are formed by calcium (or other divalent cations) cross-linking between free carboxyl groups, similar to the egg-box model of alginate gelling mechanism. Although sugar is not essential for gel formation as in HM-pectins, the presence of small amounts of sugar (10–20%) tends to decrease syneresis and adds certain firmness to these gels [61,62]. When sugar is present, the amount of divalent cation required to form gel is reduced. However, high concentrations of sugar (≥60%) prevent the gel formation because the dehydration of the sugar promotes hydrogen bonding and decreases cross-linking by divalent ion forces [62].

In this study, a HM-pectin was used, so its gelling mechanism mainly depended on the pH (acidic medium) and the presence of sugars or other solids. Gel formation was caused by hydrogen bonding between free carboxyl groups on the pectin molecules and also between the hydroxyl groups of neighboring molecules. Moreover, hydrophobic forces between methoxyl groups of different pectin chains were also established. In a neutral or only slightly acidic dispersion of pectin molecules, most of the unesterified carboxyl groups were present as partially ionized salts [60,63]. The ionized carboxylic groups produced a negative charge on the molecule, which together with the hydroxyl groups caused it to attract layers of water. The repulsive forces between those groups, due to their negative charge, could be sufficiently strong to prevent the formation of a pectin network. When citric acid was added, the COO^- groups were converted to mostly unionized carboxylic acid groups. Therefore, decreasing the number of negative charges reduced the attraction between pectin and water molecules, as well as the repulsive forces between pectin chains. The developed pharma-ink also contained sugar in the form of sucrose which contributed to the decrease in hydration of the pectin by competing for water. These conditions decreased the ability of pectin to stay in a dispersed state. When the solution was cooled at acidic pH, the chains could associate and form a gel since the network of pectin trapped the aqueous solution. However, it was reported that an excessively low pH level might cause rapid gelling without sufficient organization, resulting in a weak and poorly organized gel [60]. In general, HM-pectins show greater stability at pH = 3.5–4.0 [58,62], and the prepared hydrocortisone pharma-inks (pH 3.99 ± 0.27) were within this range of pH.

In addition, gels based on HM-pectins exhibit thermal reversibility, meaning they can undergo gel-to-sol transitions with changes in temperature [60]. At room temperature, the hydrocortisone pharma-inks were semi-solid due to the viscosity and did not flow, however, once heated to 50 °C a reduction in viscosity enabled printing. Once the layers were deposited onto the platform, the gel rapidly solidified at room temperature and successive layers could be deposited onto the previously printed layer, preventing collapse of the object.

3.2. Validation of 3DP process

The M3DIMAKER Studio software allowed the scaling of the initial 3D model size (dimensions of 10 × 10 × 4 mm) to produce four different sizes of different masses. The recorded weights after printing of these scaled objects ranged from 250 mg to 2,000 mg. The software successfully established a relationship between the scaling of the 3D model, the printing parameters employed, and the resulting masses of the printlets, which allowed the printing of dosage forms with tailored weights and doses through a new printing process.

Chewable printlets containing personalized doses ranging from 1 to 6 mg hydrocortisone were successfully printed at 50 °C through this new integrated printlet scaling approach (Figure 2). The printlets containing 1 mg exhibited lower resolution compared to printlets with higher doses. This may be attributed to the small dimensions of the 1 mg printlets relative to the 1.2 mm nozzle diameter used to print, resulting in decreased resolution for the smaller objects. The printing process was fast, requiring less than 1 min per printlet for 1–4 mg doses and less than 2 min per printlet in 5 and 6 mg doses. The appearance of the printlets could be improved if a nozzle with a lower inner diameter was used. However, the printing speed was prioritized over the resolution. In addition, the printlets were chewable, making them more attractive for pediatric patients compared to other types of formulations [27].

Flavoring and coloring agents were used to improve the acceptability of chewable printlets by the pediatric patients.

Figure 2. Image of hydrocortisone-loaded chewable printlets containing 1–6 mg, with increasing dose from left to right. The first, second, and third rows correspond to orange-green, banana-yellow and strawberry-red chewable printlets, respectively. Scale in cm.

Pharmaceutical excipients for the formulations should be chosen appropriately and carefully, avoiding any excipients that are not recommended for children [64]. In this study, these substances were provided by authorized laboratories that have products suitable for pharmaceutical compounding and can be used to prepare pharmaceutical products. Moreover, the lowest level necessary to achieve the desired effect was used (e.g. color or flavor). In any case, the established limits stated in official documents of the European Commission were not exceeded [65–67].

3.3. Mass uniformity test

After the printing process, 20 printlets were individually weighed using an analytical balance to assess any deviations from the expected printlet masses (Table 3). The Coefficient of Variation (CV) was higher for the 1 mg batch and decreased with the increase in printlet mass. This may be attributed to the small dimensions of the 1 mg printlets and the relatively large nozzle diameter of 1.2 mm in comparison, resulting in decreased resolution for the smaller printlets.

According to the Ph. Eur [44], the accepted deviation is 5% above or below the declared mass for each of the individually weighed solid dosage forms, as all printlets are equal to above 250 mg in mass. Figure 3 shows the mass distributions of each batch of printlets along with an indication of upper and lower acceptance limits from Ph. Eur.

Table 3. Dimensions and weights of each printed batch ($n = 20$).

Batch	Width (mm)	Height (mm)	Weight (mg)	CV weight (%)
1 mg	8.10 ± 0.72	2.05 ± 0.39	252.95 ± 6.91	2.73
2 mg	9.95 ± 0.39	3.00 ± 0.46	501.45 ± 8.67	1.73
3 mg	11.65 ± 0.50	3.55 ± 0.51	754.75 ± 11.70	1.55
4 mg	13.00 ± 0.32	4.35 ± 0.59	1000.90 ± 15.27	1.52
5 mg	14.15 ± 0.37	5.55 ± 0.51	1231.40 ± 18.48	1.50
6 mg	16.75 ± 0.44	5.95 ± 0.60	1530.00 ± 22.61	1.48

Results are shown as mean ± standard deviation. CV is the coefficient of variation.

All batches of the chewable printlets were within the acceptance limits (Figure 3). For the 5 and 6 mg printlets, the recorded masses were generally slightly below or above the targets, respectively. This may be corrected in the future through the software or employment of smaller nozzle diameters for more precise dispensing of material.

The chewable printlets that passed the mass uniformity test were placed in Class B X-Large amber PVC blisters. The Ph. Eur. monograph on mass uniformity testing stated that 20 dosage

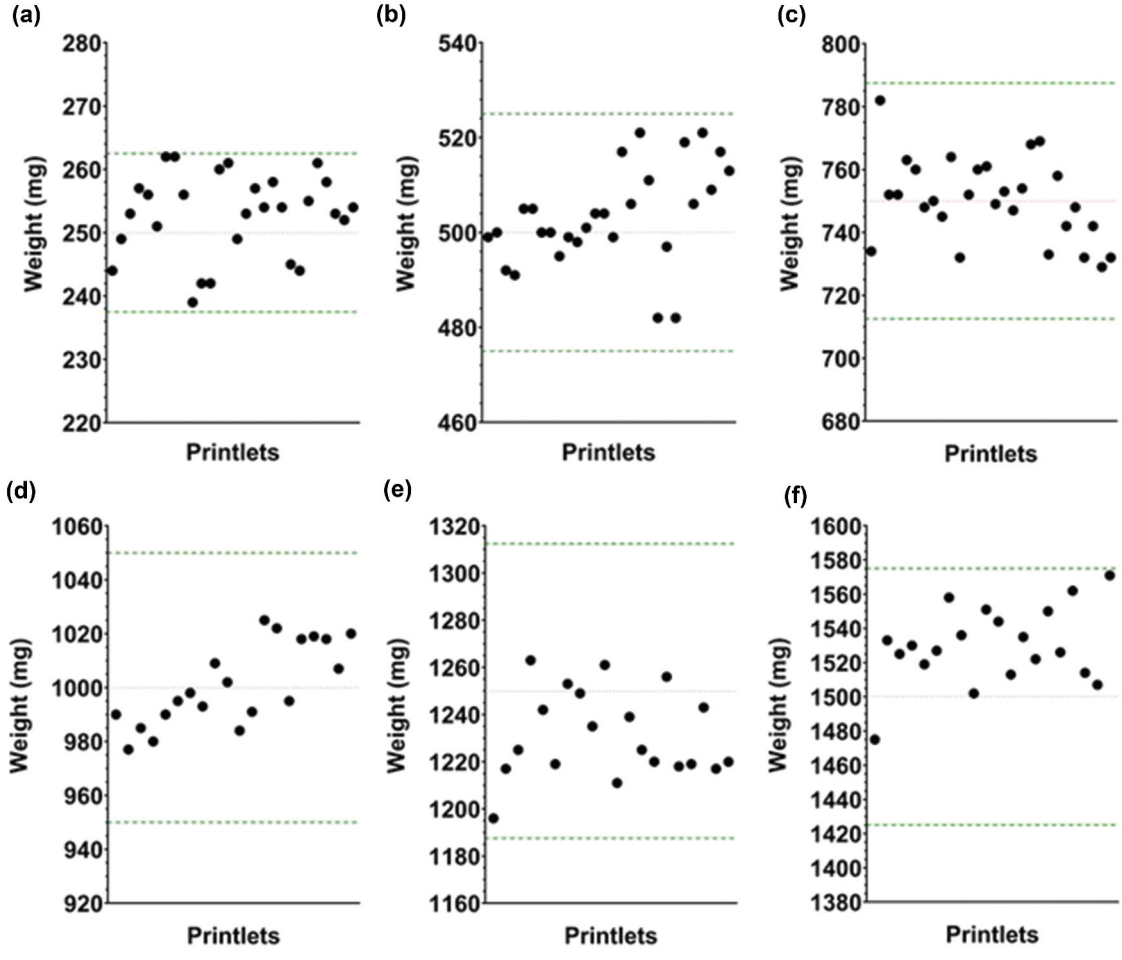

Figure 3. Recorded weights of printlets ($n = 20$) after printing process of: (a) 1 mg dose, (b) 2 mg dose, (c) 3 mg dose, (d) 4 mg dose, (e) 5 mg dose and, (f) 6 mg dose. The red dotted line refers to the declared average weights (250 mg, 500 mg, 750 mg, 1000 mg, 1250 mg, and 1500 mg, respectively), and the green lines indicate the acceptance limits of ±5%.

forms must be weighed. However, as the aim of this work was to validate a 3DP process for implementation in a hospital environment for the on-demand manufacturing of personalized medicines during a clinical trial, scenarios may be encountered where a patient would need less than 20 printlets of an identical dose strength. Therefore, all the manufactured printlets might need to be weighed to ensure their quality, which may end up being a time-consuming workflow. Recently, a 3DP system with an integrated balance was developed to perform in-line mass uniformity testing and demonstrated promising results to accelerate this quality control assay required for oral solid dosage forms [68]. The integrated system was able to weigh each individual printlet right after printing and detect any deviations from the declared weight immediately which may save time and resources. After further research and validation, the in-line weighting system may be integrated into the pharmaceutical 3D printers, being beneficial for the quality control of personalized medicines at the point-of-care (PoC).

3.4. Characterization of chewable printlets

3.4.1. X-ray powder diffraction (XRPD)

XRPD analyzes were performed to determine the solid-state of hydrocortisone in the printlet and the pharma-ink (Figure 4).

The XRPD diffractogram of the printlet showed peaks at 40° and 45° 2θ that can be attributed to sodium potassium tartrate. Moreover, the printlet exhibited peaks at 10°, 12°, 14°, and 35° 2θ that can be attributed to sucrose. The peaks at 17°, 27°, and 35° 2θ can also be attributed to sucrose. Peaks observed at 15° and 17° 2θ in the pharma-ink's and printlet's diffractograms may be attributed to hydrocortisone based on their 2θ angles and relative intensities. This indicates that hydrocortisone may be, at least partially, dispersed in the crystalline state. The intensities of both peaks were lower in the printlet compared to the pharma-ink, suggesting that the printing process may have solubilized hydrocortisone to a higher degree. Therefore, the diffractograms suggested that hydrocortisone was partially molecularly dispersed in the printlets, although there is a possibility that the low hydrocortisone concentration (0.4% w/w) may not result in crystalline diffractions even if the utilized equipment has been reported capable of detecting crystallinity down to 0.2% w/w [69].

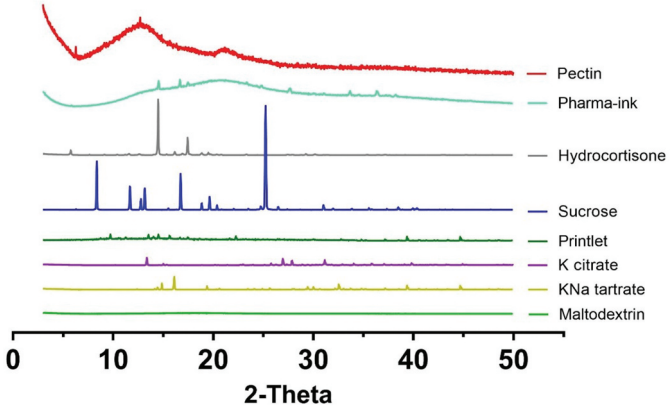

Figure 4. X-ray powder diffractograms of pure hydrocortisone and excipients, pharma-ink and printlet.

3.4.2. FTIR

FTIR was performed to clarify any possible chemical interactions between the drug and the excipients, mainly pectin, during the printing process (Figure 5).

The main characteristic peaks of the pectin could be observed [63,70,71]. The O-H stretching vibration from intra- and intermolecular hydrogen bonds of D-galacturonic acid caused a broad and strong peak at around 3200–3600 cm^{-1}. This band could be observed in pure pectin and the printlet samples. However, this broad and strong peak could be overlapped in the printlet sample due to the maltitol and maltodextrin. A peak between 2800–3000 cm^{-1} corresponds to C-H vibration and to the stretching vibration of methyl group of the methyl ester. The peak at 1750 cm^{-1} was caused by the absorption of C=O stretching vibration of methyl esterified groups and COOH groups. This peak was also observed in the printlet sample, but it was shifted. The stretching vibration of carboxylate group (COO^-) exhibited a peak at 1630 cm^{-1}. The region between 800 and 1300 cm^{-1} is related to the fingerprint region of pectin and depends on pectin type. The FTIR results suggested that no chemical interactions between hydrocortisone and excipients were encountered, although interaction signals arising from hydrocortisone may be overlapped due to the low hydrocortisone content.

3.5. Hydrocortisone content in chewable printlets

The hydrocortisone contents of the different printed batches (1–6 mg doses) are reported in Table 4. The drug loading was close to the theoretical load of 0.4% w/w.

According to the Ph. Eur., the content uniformity test of single-dose preparations is based on the assessment of the individual content of the drug of the single-dose units, to determine if the individual contents are within the established limits with respect to the average claimed [49]. Using an appropriate analytical method, the individual drug content in 10 samples per batch taken at random must be determined. In this study, individual content of 10 printlets prepared per batch was evaluated (using the HPLC-UV method described in Section 2.7) to determine any deviations in the content of each printlet. The Ph. Eur. states that the batch is accepted if each individual content is between 85% and 115% of the average content. The batch does not comply with the assay if more than one individual content is outside these limits or if one individual content is outside the limits 75% to 125% of the mean content. In this study, all printed batches were within the acceptance limits, and the hydrocortisone content was 100% (Table 4). This ensured that all the 3D printed formulations contained the declared amount of hydrocortisone and that there was no drug degradation during printing. Moreover, for the lowest and the highest doses, no deviations in the drug content were found between the three printed batches and the mean value of the three batches' contents. The Kruskal–Wallis test was performed to elucidate whether there were inter-batch differences between hydrocortisone contents and whether there were differences in

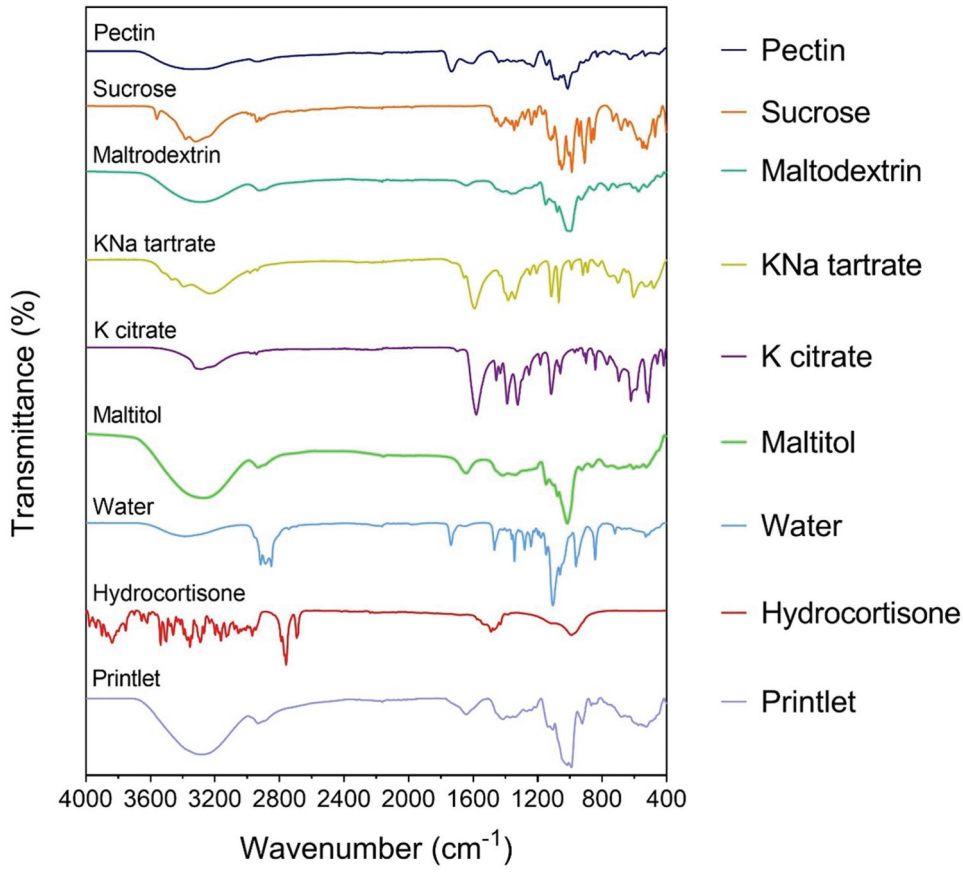

Figure 5. FTIR spectra of the excipients, hydrocortisone, and the chewable printlet.

hydrocortisone content between batches printed at the time of production and after 1 month of storage. No significant differences were found in either case ($p > 0.05$).

3.6. Mechanical properties of chewable printlets

Currently, there are no established acceptance criteria for hardness in chewable tablets although the FDA recommends (non-binding recommendation) values less than 12 kp, equivalent to 118 N. In the mechanical study, the printlet was initially compressed until a 65 N force was reached as this has been reported the minimum masticatory force for children aged 7 −10 years [72]. The printlet exhibited an elastic behavior at 65 N force and the printlet was not broken after five cycles and fully recovered the shape at removal of force. The Young's modulus recorded was 1.45 MPa.

When the applied force was increased to 80 N, the printlet did not break after five compression cycles but was slightly deformed when the force was removed. The Young's modulus in the first linear region of the stress-strain plot was 2.15 MPa. The tests at a compression force of 100 N and 120 N, values close to the FDA recommended ones, caused the printlets to break in the first cycle.

The area under the stress–strain curve (AUC) values were calculated for the first cycle for 65 N, 80 N, 100 N, and 120 N (Figure 6). The higher the value of the AUC, the greater the energy absorption capacity before deformation. The AUC for tests carried out applying 65 N and 80 N was practically the same in all cycles, indicating good elasticity maintaining capability to absorb energy without deformation. The printlets tested at 120 N force exhibited less energy absorption capacity before deforming than at 100 N.

The chewing difficulty index (CDI) values (calculated using Equation 1 in Section 2.8) were 0.5 Nm and 0.6 Nm for 100 N and 120 N applied forces, respectively. The CDI has recently been proposed as a quantitative measurement of the ease or difficulty of chewing a chewable tablet [25]. The CDI of lanthanum carbonate chewable tablets ranged from 0.09 Nm to 1.24 Nm, depending on the hardness of the printlet and the exposition time to saliva [73]. The CDIs were also obtained for chewable antacid tablets (0.30–0.81 Nm) and chocolate-flavored dexamethasone tablets (0.87–0.91 Nm) and the results depended on the hardness and the type of tablet [74,75]. The CDI of the 3D printed and

Table 4. Hydrocortisone content results performing in the different printed batches of 1–6 mg doses.

Batch	Hydrocortisone content (% w/w)	Hydrocortisone content after 1 month (% w/w)
1 mg	100.12 ± 1.76	100.42 ± 1.92
2 mg	101.08 ± 1.47	–
3 mg	100.71 ± 0.76	–
4 mg	99.66 ± 1.23	–
5 mg	99.76 ± 1.34	–
6 mg	100.07 ± 1.18	100.50 ± 1.67

Results are shown as mean ± standard deviation.

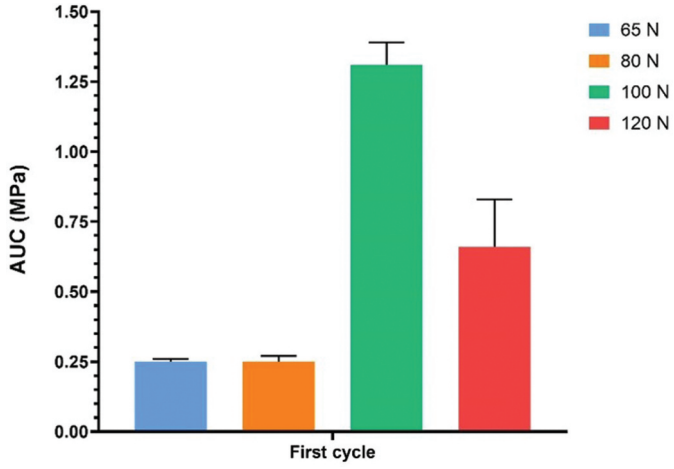

Figure 6. Values of the area under the stress–strain curve (AUC) in the first compression cycle of the printlets under 65 N, 80 N, 100 N and 120 N compression forces.

molded chocolate dosage forms ranged between 0.15 and 0.28 Nm [76]. Therefore, the CDI values of the developed hydrocortisone printlets were in line with previously reported chewable tablets and may reduce even further after exposure to patient saliva, further aiding chewing.

3.7. In vitro *dissolution test*

Hydrocortisone release profiles from the printlets in pH = 1.2, pH = 4.5, pH = 6.8 and pH = 6.9 (distilled water) media are shown in Figure 7(a–d), respectively. The dissolution tests were carried out for printlets containing the lowest dose (1 mg) and for printlets containing the highest dose (6 mg).

The printlets reduced in size over time during the different dissolution test conditions. Thus, the main mechanism contributing to the release was erosion regardless of the pH, and the drug was progressively released from the dosage form as it eroded. Relevantly, the release from the 1 mg printlets was faster than from the 6 mg printlets in all dissolution media due to the larger surface area to volume (SA/V) ratio of the former. Each dosage form had a different SA/V ratio because of their different dimensions (1 mg: 0.50 ± 0.00 SA/V and 6 mg: 0.16 ± 0.01 SA/V), resulting in different drug release rates.

At pH = 1.2, approximately 97% (1 mg printlet) and 85% (6 mg printlet) of the drug were released at 30 min. At pH = 4.5, approximately 98% (1 mg printlet) and 92% (6 mg printlet) of the drug were released at 30 min. Approximately 96% (1 mg printlet) and 89% (6 mg printlet) of the drug were released at pH = 6.8. In water (as USP monograph states), 100% (1 mg printlet) and 88% (6 mg printlet) of hydrocortisone were released. In the USP monograph regarding the dissolution test of hydrocortisone tablets [46], the dissolution test conditions for conventional hydrocortisone tablets recommends to carry out the assay in 900 ml of water, hence why this assay was performed here. The USP establishes as a tolerance limit that '*no less than 70% should dissolve in the first 30 min*.' At 30 min, both 1 and 6 mg printlets reached approximately 90–100% hydrocortisone dissolution independent of SA/V ratio, thus complying with the dissolution test specifications according to USP.

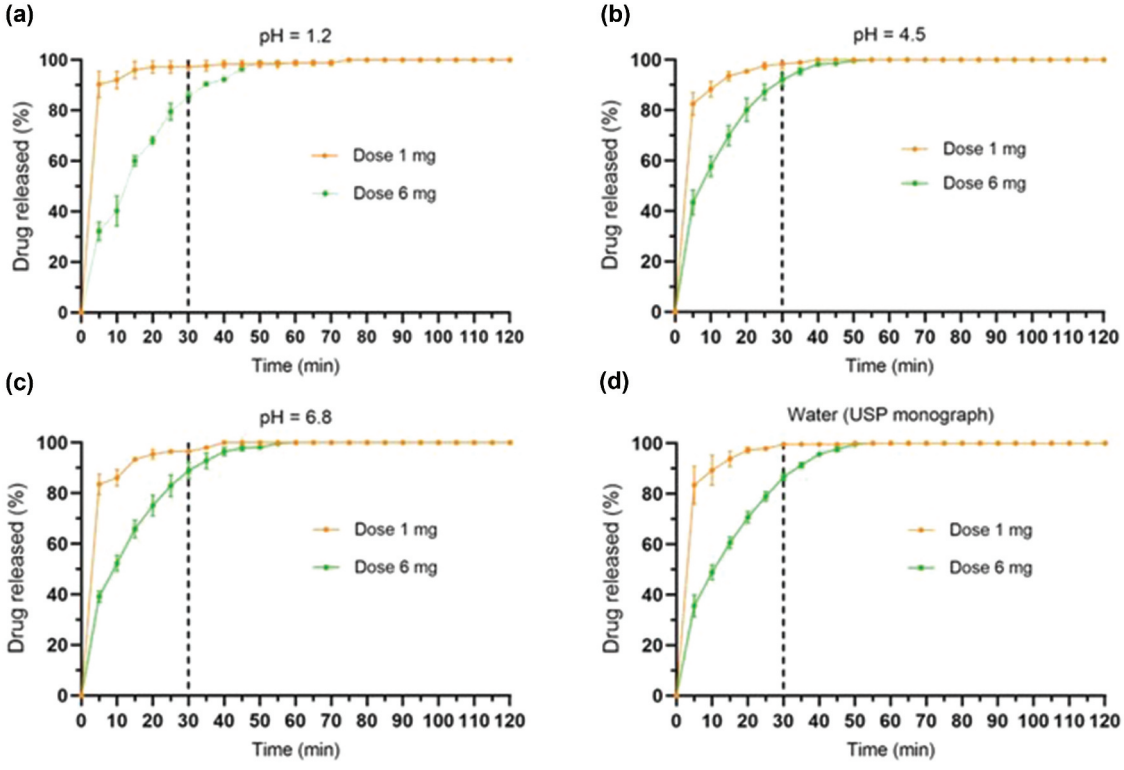

Figure 7. Hydrocortisone release profiles from chewable printlets at different pH (37°C, USP-II apparatus): (a) 1.2; (b) 4.5; (c) 6.8; and (d) water (according to the USP monograph for hydrocortisone tablets). The black dashed line indicated the 30 min point of the assay.

According to the Ph. Eur., conventional immediate release dosage forms should release at least 80% of the active substance within a specified time, typically 45 min or less [77]. In total, 100% of hydrocortisone was released from both 1 and 6 mg printlets within 45 min (Figure 7). Therefore, the printlets may be considered as immediate release dosage forms according to Ph. Eur.

Notably, standard dissolution tests and conditions for chewable tablets are still unavailable in Pharmacopoeias, and it is recommended by the FDA to follow and perform the dissolution tests specified for conventional tablets [45]. The FDA recommends carrying out the experiments using intact tablets and that it is advisable that chewable tablets meet the same dissolution specifications as immediate-release tablets [45]. The chewable printlets prepared using the SSE printhead complied with the USP monograph for hydrocortisone tablets as well as the immediate-release recommendations stated by the EMA [46,77]. However, it should be noted that these testing conditions do not mimic realistic or physiological conditions as chewable printlets would be chewed into smaller particulates before swallowing, potentially enhancing the dissolution rate due to drastically increased SA/V.

3.8. Stability test in chewable printlets

The individual content of 1 and 6 mg printlets from three different batches were determined to be within the established limits after 1 month of storage in blisters under the storage conditions of 30 °C and 65% relative humidity.

The individual contents of all evaluated printlets were between 85% and 115% of the declared content (Table 4), thus complying with the established limits specified in Ph. Eur. for content uniformity. Based on the results (Table 4), the stability of the chewable printlets under the mentioned storage conditions was set for 1 month. This time frame would be sufficient to carry out clinical trials in pediatric patients.

Degradation of hydrocortisone was not expected during the production process of the pharma-ink, as hydrocortisone exhibits thermal degradation above 220 °C [78], almost three times higher than the temperature applied during the pharma-ink preparation. The available literature on temperature stability data for hydrocortisone is conclusive. One study evaluated the stability of a 2.5% w/w hydrocortisone cream stored in a vial for 3 days at 80 °C with no detected degradation products [79]. Another study conducted a thermal degradation investigation on marketed 50 mg hydrocortisone tablets [80]. Samples were exposed to dry heat in an oven at 100 °C for 2 h. In total, 17% of hydrocortisone was degraded and small peaks of impurities were detected under these extreme conditions of temperature and exposure times.

In a study where hydrocortisone printlets were prepared using fused-deposition modeling (FDM) 3DP technology, the hot melt extrusion (HME) and 3DP temperatures were 150 °C [81]. Stability studies were performed for 1 month according to the ICH Guidelines, and an impurity study was also carried out due to the processing temperatures. Impurities were observed, and they were related to the exposure time during filament formation by HME and the FDM 3D printing process at 150 °C. The authors noted that an alternative to reduce and avoid the risk of drug degradation and impurity formation is to use SSE 3DP technology. The temperature during the production of the pharma-ink mentioned in the present work was only 80 °C momentarily before reduction to 60 °C, and along with an overall decrease in heat exposure time, the thermal degradation of hydrocortisone may be negligible minimizing the risk of thermal hydrocortisone degradation. This was confirmed upon the stability study as the observed hydrocortisone content after 1 month of storage was the same as the initial one with no statistical differences ($p > 0.05$) (Table 4). In addition, no degradation products were detected in the HPLC chromatograms.

3.9. Technical information on pharma-ink and printlets required by the AEMPS

Currently, no established regulatory framework for the manufacture of medicines using 3D printing exists. The FDA, Medicines and Healthcare products Regulatory Agency (MHRA), and EMA are taking tangible steps to adapt the regulatory frameworks to 3DP [82–85]. For instance, the FDA has published a paper evaluating the existing risk-based regulatory framework applicable to PoC manufacturing, identifying challenges and proposing future initiatives in this domain [83]. In addition, the MHRA has proposed a regulatory framework for products produced at the PoC concerning medicine approvals, clinical trials, and regulatory compliance evaluations, enhancing the safety and effectiveness of the medicines [84]. Harmonization of these regulatory frameworks is not possible due to the differing legislation between countries and sometimes between autonomous regions within the same country, as is the case for Spain and its Autonomous Communities. Here, we provide an overview of the basic information demanded by the AEMPS in terms of pharma-ink and 3DP tablets for approval to conduct the clinical trial (Table 2). This may serve as a guideline for required information by other local regulatory agencies for the development and planning of future clinical trials on 3DP tablets.

The chewable 3DP medicines containing personalized doses were characterized in terms of physicochemical status, drug content, *in vitro* release profiles, and stability in order to ensure the quality of chewable medicines and comply with the requirements before conducting the clinical trial in children. Presentation of physicochemical and rheological data was not mandatory by AEMPS; therefore, part of the data presented in this article was not strictly required.

One of the AEMPS's main concerns was around the novelty and safety of the pharma-ink. Hence, it was important to prove that the excipients used to prepare the pharma-ink are commonly used pharmaceutical excipients and were purchased from authorized suppliers. Furthermore, data from the previous two clinical studies using similar chewable 3DP formulations containing isoleucine, valine, isoleucine-valine combination, and citrulline instead of hydrocortisone provided reassurance to the agency [38,39].

Another concern was around the 'candy-likeness' of the final printlets as this could result in an undesirable medication usage among the children. Several arguments to justify the usage of these novel dosage forms were presented. First, the

doses of hydrocortisone in the replacement therapy included in this clinical trial to restore normal cortisol concentrations were low (1–6 mg). Therefore, the profile of adverse reactions due to intoxication would not be comparable to those observed in other pathologies that require much higher doses of oral glucocorticoids. Second, we indicated that the EMA document '*Guideline on pharmaceutical development of medicines for pediatric use*' was followed. Here, researchers are encouraged to develop formulations appropriate for children, propose alternative dosage forms, and other strategies taking into account various aspects that impact acceptability and, therefore, adherence to treatment [86]; however, it is also stated that the medication should not be 'candy-like' to avoid misuse. The active ingredient in this study, hydrocortisone base, is a bitter tasting ingredient. The bitter taste will be partially masked with sucrose and flavoring due to the low levels of hydrocortisone, however the taste will not be masked completely as a consequence of the inherent bitterness of the active ingredient. The chewable printlets should not be attractive enough in terms of flavor; hence, medication misuse by the children is not expected. Third, an aim of the clinical trial is also to assess the acceptability of the chewable printlets compared to the medication from conventional compounding. Lastly, warnings were added ('Keep out of the reach of children') to the exterior of the final blister packaging of the product as well as recommendations for the parents and/or guardians to control the administration of the medication to make it inaccessible by the children directly.

The novelty of the 3DP process was another concern highlighted. The 3DP process consisted of an automatization of the conventional pharmaceutical compounding to ensure the reproducibility and safety of the final formulations. The Standard Operating Procedure (SOP) for the preparation of the pharma-ink was extensively described in the documents submitted to AEMPS for reproducibility of the elaboration process. The preparation process was repeated several times with the same equipment that will be available in the hospital's Pharmacy Service to ensure the reproducibility and avoid deviations. It was critical to describe in detail the 3DP process as most regulatory agencies are not familiar with these innovative technologies and the evidence from clinical studies is scarce. An SOP describing the preparation of chewable printlets using the 3D printer and integrated software for specification of target dose and number of dosage forms to print was essential. All the printing parameters (i.e. extrusion temperature) needed to be well defined to ensure a consistent and reproducible manufacturing process for dosage forms with the desired quality. The 3DP process needed to be validated under certain conditions (temperature and printing speed) to prove the possibility of preparing the range of doses that will be printed during the clinical trial.

It was mandatory to show uniformity of mass and that the tablets did not present deviations attributed to the 3DP process. Therefore, the mass of each chewable printlet needed to comply with the Ph. Eur. acceptance limits [44]. The uniformity of content of single-dose preparations must be assessed using a proper analytical method to determine if the individual contents were within the established limits with respect to the average claimed [49]. In addition, it was vital to determine if there were impurities in the printlets that may appear during pharma-ink elaboration or the printing process.

The evaluation of drug release at different conditions was crucial [77,87]. Hydrocortisone release from the chewable printlets was evaluated at three different pH conditions as specified in the EMA guidelines for biowaiver for bioequivalence studies, which is currently only applicable to Biopharmaceutics Classification System (BCS) Class I and III drugs [88]. Hydrocortisone belongs to Biopharmaceutics Drug Disposition Classification System (BDDCS) Class I and may be considered equal to BCS Class I drugs in terms of solubility [89]. BDDCS drugs are classified according to intestinal permeability rate rather than extent of absorption, but these parameters have been proven highly correlated, and this evidence was approved for the clinical trial. Drug release was also evaluated under the conditions of the USP monograph for hydrocortisone tablets to prove that the printlets would comply with compendial requirements.

A stability study was crucial to prove that the printlets were stable during storage for the duration of the clinical trial, and it needed to be performed according to ICH Guidelines [47]. In this case, the duration of the treatment in the trial is maximum 1 month, hence the stability study was designed accordingly. Literature data related to degradation of the drug under different conditions was provided to support the experimental data and was appreciated by the regulatory agency.

Significant contamination (including microbiological) must be avoided during the elaboration of pharma-ink and 3DP processes. The 3DP medicines will be manufactured in the cleanroom of the hospital, and it is vital to ensure and demonstrate microbiological control during the clinical trial using a compendial method [90–92].

The potential and promising outcomes of 3D printing technologies, both in hardware and software, have facilitated the implementation of hospital-based 3DP of medication, reducing processing times, costs, and a move toward more accessible personalized medicine. The absence of a regulatory framework or specific guidelines for individual legislative regions for the development of pharmaceutical 3DP medicines can be attributed to the novelty and rapid advancement of the technology, however it does not hinder its implementation. As such, gathering real clinical evidence and data on 3DP dosage forms is essential to facilitate the actual implementation of this technology in healthcare services.

4. Conclusions

In this work, chewable 3DP tablets containing hydrocortisone were developed and extensively characterized for the purpose of carrying out an imminent clinical trial in the Vall d'Hebron Hospital (EudraCT: 2021-001069-20 and NCT: NCT06435481) located in Barcelona, Spain. The pharma-inks were prepared using three different flavors and colors to improve the palatability, acceptability, and thereby adherence to the treatment of future pediatric patients. The 3DP process was validated using the M3DIMAKER Studio software. The hydrocortisone content was approximately 100%, ensuring that the patients will receive the individually prescribed doses during the clinical trial. The hydrocortisone release from the chewable

printlets was immediate and the amount released complied with specifications from both Ph. Eur. and USP. The chewable printlets were stable for 1 month of storage with no chemical degradation observed.

Moreover, personalized doses ranging from 1 to 6 mg hydrocortisone could be prepared simply and easily using the specific healthcare software. Doses between the printed ones in this study may be prepared on-demand during the clinical trial through the software wizard, further highlighting the versatility of 3DP technologies for personalized medicines.

Lastly, the technical information on the 3DP manufacturing process and quality of the pharma-ink and printlets required by the AEMPS for the approval to conduct the clinical study has been presented here. While this specific study was approved by the Spanish authorities, the basic information required would likely be identical between different local regulatory authorities. Hence, this compilation may serve as a starting point and guideline for healthcare professionals seeking to develop 3DP medicines to conduct clinical trials across different regulatory regions.

Funding

This paper was funded by the UK Research and Innovation, the Engineering and Physical Sciences Research Council [EP/S023054/1], and the Ministerio de Universidades [FPU20/01245].

Declarations of interest

AW Basit reports a relationship with FABRX Ltd. that includes equity. A Goyanes reports a relationship with FABRX Ltd. that includes equity. The authors have no other relevant affiliations or financial involvement with any organization or entity with a financial interest in or financial conflict with the subject matter or materials discussed in the manuscript apart from those disclosed.

Reviewer disclosures

Peer reviewers on this manuscript have no relevant financial or other relationships to disclose.

Author contributions

L Rodríguez-Pombo: Conceptualization, Data curation, Formal Analysis, Investigation, Methodology, Visualization, Funding acquisition, Writing – original draft, and Writing – review and editing. **C Gallego-Fernández**: Data curation, Formal analysis, Investigation, and Visualization. **AK Jørgensen**: Writing – review and editing, Writing – original draft, Validation, and Formal analysis. **CJ Parramon-Teixidó**: Methodology, Investigation, and Validation. **C Cañete-Ramirez**: Conceptualization, Methodology, Investigation, and Validation. **MJ Cabañas-Poy**: Conceptualization, Methodology, Investigation, Validation, and Writing – review and editing. **AW Basit**: Writing – review and editing, Visualization, Supervision, Resources, Project administration, and Conceptualization. **C Alvarez-Lorenzo**: Supervision, Resources, Writing – review and editing, Conceptualization, Methodology, Project administration, Visualization, Formal analysis, and Investigation. **A Goyanes**: Conceptualization, Supervision, Resources, Writing – review and editing, Methodology, Validation, and Project administration.

ORCID

Carlos Javier Parramon-Teixidó http://orcid.org/0000-0001-8023-3979
Carmen Alvarez-Lorenzo http://orcid.org/0000-0002-8546-7085

References

Papers of special note have been highlighted as either of interest (•) or of considerable interest (••) to readers.

1. Hahner S, Ross RJ, Arlt W, et al. Adrenal insufficiency. Nat Rev Dis Primers. 2021;7(1):19. doi: 10.1038/s41572-021-00252-7
2. Husebye ES, Pearce SH, Krone NP, et al. Adrenal insufficiency. Lancet. 2021;397(10274):613–629. doi: 10.1016/S0140-6736(21)00136-7
3. Arlt W, Allolio B. Adrenal insufficiency. Lancet. 2003;361(9372):1881–1893. doi: 10.1016/S0140-6736(03)13492-7
4. White PC, Speiser PW. Congenital adrenal hyperplasia due to 21-hydroxylase deficiency. Endocr Rev. 2000;21(3):245–291. doi: 10.1210/edrv.21.3.0398
5. Mohd Azmi NAS, Juliana N, Azmani S, et al. Cortisol on circadian rhythm and its effect on cardiovascular system. Int J Environ Res Public Health. 2021;18(2):676. doi: 10.3390/ijerph18020676
6. Chan S, Debono M. Review: replication of cortisol circadian rhythm: new advances in hydrocortisone replacement therapy. Ther Adv Endocrinol Metab. 2010;1(3):129–138. doi: 10.1177/2042018810380214
7. Nisticò D, Bossini B, Benvenuto S, et al. Pediatric adrenal insufficiency: challenges and solutions. Ther Clin Risk Manag. 2022;18:47–60. doi: 10.2147/TCRM.S294065
• **of interest.**
8. Speiser PW, Arlt W, Auchus RJ, et al. Congenital adrenal hyperplasia due to steroid 21-hydroxylase deficiency: an endocrine Society clinical practice guideline. J Clin Endocrinol Metab. 2018;103(11):4043–4088. doi: 10.1210/jc.2018-01865
9. El-Maouche D, Arlt W, Merke DP. Congenital adrenal hyperplasia. Lancet. 2017;390(10108):2194–2210. doi: 10.1016/S0140-6736(17)31431-9
10. EMA. Plenadren product information. 2017 Jan [cited 2023 Sep 18]; Available from: https://www.ema.europa.eu/en/documents/product-information/plenadren-epar-product-information_en.pdf
11. EMA. Efmody product information. 2023 Aug [cited 2023 Sep 18]; Available from: https://www.ema.europa.eu/en/documents/product-information/efmody-epar-product-information_en.pdf
12. EMA. Alkindi product information. 2023 [cited 2023 Sep 18]; Available from: https://www.ema.europa.eu/en/documents/product-information/alkindi-epar-product-information_en.pdf
13. Whitaker MJ, Spielmann S, Digweed D, et al. Development and testing in healthy adults of oral hydrocortisone granules with taste masking for the treatment of neonates and infants with adrenal insufficiency. J Clin Endocrinol Metab. 2015;100(4):1681–1688. doi: 10.1210/jc.2014-4060
14. Saito J, Yoshikawa N, Hanawa T, et al. Stability of hydrocortisone in oral powder form compounded for pediatric patients in Japan. Pharmaceutics. 2021;13(8):1267. doi: 10.3390/pharmaceutics13081267
15. Pramar YV, Mandal TK, Bostanian LA, et al. Physicochemical and microbiological stability of extemporaneously compounded hydrocortisone oral suspensions in PCCA base, SuspendIt. Int J Pharm Compd. 2021;25(5):431–439.
16. Watson CJ, Whitledge JD, Siani AM, et al. Pharmaceutical compounding: a history, regulatory overview, and systematic review of compounding errors. J Med Toxicol. 2021;17(2):197–217. doi: 10.1007/s13181-020-00814-3
17. Neumann U, Burau D, Spielmann S, et al. Quality of compounded hydrocortisone capsules used in the treatment of children. Eur J Endocrinol. 2017;177(2):239–242. doi: 10.1530/EJE-17-0248
18. Bonfig W, Dalla Pozza SB, Schmidt H, et al. Hydrocortisone dosing during puberty in patients with classical congenital adrenal hyperplasia: an evidence-based recommendation. J Clin Endocrinol Metab. 2009;94(10):3882–3888. doi: 10.1210/jc.2009-0942
19. Grigorescu-Sido A, Bettendorf M, Schulze E, et al. Growth analysis in patients with 21-hydroxylase deficiency influence of glucocorticoid dosage, age at diagnosis, phenotype and genotype on growth

and height outcome. Horm Res Paediatr. 2003;60(2):84–90. doi: 10.1159/000071876
20. Nadagouda MN, Rastogi V, Ginn M. A review on 3D printing techniques for medical applications. Curr Opin Chem. 2020;28:152–157. doi: 10.1016/j.coche.2020.05.007
21. Vaz VM, Kumar L. 3D printing as a promising tool in personalized medicine. AAPS PharmScitech. 2021;22(1):49. doi: 10.1208/s12249-020-01905-8
22. Serrano DR, Kara A, Yuste I, et al. 3D printing technologies in personalized medicine, Nanomedicines, and biopharmaceuticals. Pharmaceutics. 2023;15(2):313. doi: 10.3390/pharmaceutics15020313
23. Andreadis II, Gioumouxouzis CI, Eleftheriadis GK, et al. The advent of a new era in digital healthcare: a role for 3D printing technologies in drug manufacturing? Pharmaceutics. 2022;14(3):14(3. doi: 10.3390/pharmaceutics14030609
24. Seoane-Viaño I, Alvarez-Lorenzo JP, Basit C, et al. Semi-solid extrusion 3D printing in drug delivery and biomedicine: personalised solutions for healthcare challenges. J Control Release. 2021;332:367–389. doi: 10.1016/j.jconrel.2021.02.027
• **of interest.**
25. Rodríguez-Pombo L, Awad A, Basit AW, et al. Innovations in chewable formulations: the novelty and applications of 3D printing in drug product design. Pharmaceutics. 2022;14(8):1732. doi: 10.3390/pharmaceutics14081732
26. Auriemma G, Tommasino C, Falcone G, et al. Additive manufacturing strategies for personalized drug delivery systems and medical devices: fused filament fabrication and semi solid Extrusion. Molecules. 2022;27(9):2784. doi: 10.3390/molecules27092784
27. Januskaite P, Xu X, Ranmal SR, et al. I spy with my little eye: a paediatric visual preferences survey of 3D printed tablets. Pharmaceutics. 2020;12(11):1100. doi: 10.3390/pharmaceutics12111100
• **of interest.**
28. Cui M, Pan H, Fang D, et al. Fabrication of high drug loading levetiracetam tablets using semi-solid extrusion 3D printing. J Drug Deliv Sci Technol. 2020;57:101683. doi: 10.1016/j.jddst.2020.101683
29. Cheng Y, Qin H, Acevedo NC, et al. 3D printing of extended-release tablets of theophylline using hydroxypropyl methylcellulose (HPMC) hydrogels. Int J Pharm. 2020;591:119983. doi: 10.1016/j.ijpharm.2020.119983
30. Karavasili C, Gkaragkounis A, Moschakis T, et al. Pediatric-friendly chocolate-based dosage forms for the oral administration of both hydrophilic and lipophilic drugs fabricated with extrusion-based 3D printing. Eur J Pharm Sci. 2020;147:105291. doi: 10.1016/j.ejps.2020.105291
31. Herrada-Manchon H, Rodríguez-González D, Alejandro Fernández M, et al. 3D printed gummies: personalized drug dosage in a safe and appealing way. Int J Pharm. 2020;587:119687. doi: 10.1016/j.ijpharm.2020.119687
• **of interest.**
32. Oblom H, Sjöholm E, Rautamo M, et al. Towards printed pediatric medicines in hospital pharmacies: comparison of 2D and 3D-Printed orodispersible warfarin films with conventional oral powders in unit dose sachets. Pharmaceutics. 2019;11(7):11(7. doi: 10.3390/pharmaceutics11070334
33. Yan T-T, Lv Z-F, Tian P, et al. Semi-solid extrusion 3D printing ODFs: an individual drug delivery system for small scale pharmacy. Drug Dev Ind Pharm. 2020;46(4):531–538. doi: 10.1080/03639045.2020.1734018
34. Khaled SA, Burley JC, Alexander MR, et al. 3D printing of five-in-one dose combination polypill with defined immediate and sustained release profiles. J Control Release. 2015;217:308–314. doi: 10.1016/j.jconrel.2015.09.028
35. Goh WJ, Tan SX, Pastorin G, et al. 3D printing of four-in-one oral polypill with multiple release profiles for personalized delivery of caffeine and vitamin B analogues. Int J Pharm. 2021;598:120360. doi: 10.1016/j.ijpharm.2021.120360
36. Seoane-Viaño I, Ong JJ, Luzardo-Álvarez A, et al. 3D printed tacrolimus suppositories for the treatment of ulcerative colitis. Asian J Pharm Sci. 2021;16(1):110–119. doi: 10.1016/j.ajps.2020.06.003
37. Duman G, Yıldır İ, Macit M, et al. Development and evaluation of 3D-printed ocular insert containing liposomal moxifloxacin. J Drug Deliv Sci Technol. 2024;92:105353. doi: 10.1016/j.jddst.2024.105353
38. Goyanes A, Madla CM, Umerji A, et al. Automated therapy preparation of isoleucine formulations using 3D printing for the treatment of MSUD: first single-centre, prospective, crossover study in patients. Int J Pharm. 2019;567:118497. doi: 10.1016/j.ijpharm.2019.118497
39. Rodríguez-Pombo L, de Castro-López MJ, Sánchez-Pintos P, et al. Paediatric clinical study of 3D printed personalised medicines for rare metabolic disorders. Int J Pharm. 2024;657:124140. doi: 10.1016/j.ijpharm.2024.124140
•• **of considerable interest.**
40. Lyousoufi M, Lafeber I, Kweekel D, et al. Development and bioequivalence of 3D-Printed medication at the point-of-care: bridging the gap toward personalized medicine. Clin Pharmacol Ther. 2023;113(5):1125–1131. doi: 10.1002/cpt.2870
•• **of considerable interest.**
41. Liu L, Fu K, Hong S, et al. Improving the quality and clinical efficacy of subdivided levothyroxine sodium tablets by 3D printing technology. J Drug Deliv Sci Technol. 2023;89:105008. doi: 10.1016/j.jddst.2023.105008
• **of interest.**
42. Cantalupi A, Maraschi F, Pretali L, et al. Glucocorticoids in freshwaters: degradation by solar light and environmental toxicity of the photoproducts. Int J Environ Res Public Health. 2020;17(23):8717. doi: 10.3390/ijerph17238717
43. Caffieri S, Dall'acqua S, Castagliuolo I, et al. UVB photolysis of hydrocortisone 21-acetate. J Pharm Biomed Anal. 2008;47(4–5):771–777. doi: 10.1016/j.jpba.2008.03.008
44. Europe, C.o. 2.9.5. Uniformity of mass os single-dose preparations. European pharmacopoeia. 2024 [cited 2024 Jan 7]; [Available from: https://pheur.edqm.eu/app/11-5/content/11-5/20905E.htm?highlight=on&terms=uniformity&terms=mass
45. FDA. Quality attribute considerations for chewable tablets guidance for industry. Docket number: FDA-2016-D-1490 (Silver Spring, Maryland: Center for Drug Evaluation and Research); 2020. https://www.fda.gov/regulatory-information/search-fda-guidance-documents/quality-attribute-considerations-chewable-tablets-guidance-industry
• **of interest.**
46. USP-NF. Hydrocortisone tablets. United States pharmacopeia 2023. 2023 Aug 1 [cited 2024 Jan 28]; Available from: https://usp.org/USPNF/USPNF_M38180_03_01.html
47. EMA. ICH topic Q 1 a (R2) stability testing of new drug substances and products. 2003 Aug [cited 2024 Feb 15]; Available from: https://www.ema.europa.eu/en/ich-q1a-r2-stability-testing-new-drug-substances-and-drug-products-scientific-guideline
48. WHO. Stability testing of active pharmaceutical ingredients and finished pharmaceutical products. Stability conditions for WHO member states by region. 2021 [cited 2024 Feb 15]; Available from: https://cdn.who.int/media/docs/default-source/medicines/norms-and-standards/guidelines/regulatory-standards/trs953-annex2-appendix1-stability-conditions-table-2018.pdf?sfvrsn=74032aec_12&download=true
49. Europe, C.o. 2.9.6. Uniformity of content of single-dose preparations. European pharmacopoeia. 2024 [cited 2024 Jan 7]; Available from: https://pheur.edqm.eu/internal/6d3018cf264c4ca9a2cd144ac6a14e57/11-5/11-5/page/20906E.pdf
50. Zidan A, Alayoubi A, Asfari S, et al. Development of mechanistic models to identify critical formulation and process variables of pastes for 3D printing of modified release tablets. Int J Pharm. 2019;555:109–123. doi: 10.1016/j.ijpharm.2018.11.044
51. Díaz-Torres E, Rodríguez-Pombo L, Ong JJ, et al. Integrating pressure sensor control into semi-solid extrusion 3D printing to optimize medicine manufacturing. Int J Pharm X. 2022;4:100133. doi: 10.1016/j.ijpx.2022.100133
52. Zidan A, Alayoubi A, Coburn J, et al. Extrudability analysis of drug loaded pastes for 3D printing of modified release tablets. Int J Pharm. 2019;554:292–301. doi: 10.1016/j.ijpharm.2018.11.025
53. Govender R, Kissi EO, Larsson A, et al. Polymers in pharmaceutical additive manufacturing: a balancing act between printability and

product performance. Adv Drug Deliv Rev. 2021;177:113923. doi: 10.1016/j.addr.2021.113923
54. Rahman J, Quodbach J. Versatility on demand - the case for semi-solid micro-extrusion in pharmaceutics. Adv Drug Deliv Rev. 2021;172:104–126. doi: 10.1016/j.addr.2021.02.013
55. Díaz-Torres E, Suárez-González J, Monzón-Rodríguez CN, et al. Characterization and validation of a new 3D printing ink for reducing Therapeutic gap in pediatrics through individualized medicines. Pharmaceutics. 2023;15(6):1642. doi: 10.3390/pharmaceutics15061642
56. Conceicao J, Farto-Vaamonde X, Goyanes A, et al. Hydroxypropyl-β-cyclodextrin-based fast dissolving carbamazepine printlets prepared by semisolid extrusion 3D printing. Carbohydr Polym. 2019;221:55–62. doi: 10.1016/j.carbpol.2019.05.084
57. Ropartz D, Ralet M-C. *Pectin structure*. In: Kontogiorgos V, editor. *Pectin: technological and physiological properties*. Cham: Springer International Publishing; 2020. p. 17–36.
58. Thibault JF, Ralet MC. *Physico-chemical properties of pectins in the cell walls and after extraction*. In: Voragen F, Schols H Visser R, editors. *Advances in pectin and pectinase research*. Springer Netherlands: Dordrecht; 2003. p. 91–105.
59. Li D-Q, Li J, Dong H-L, et al. Pectin in biomedical and drug delivery applications: a review. Int J Biol Macromol. 2021;185:49–65. doi: 10.1016/j.ijbiomac.2021.06.088
•• **of considerable interest.**
60. Said NS, Olawuyi IF, Lee WY. Pectin hydrogels: gel-forming behaviors, mechanisms, and food applications. Gels. 2023;9(9):732. doi: 10.3390/gels9090732
61. Lara-Espinoza C, Carvajal-Millán E, Balandrán-Quintana R, et al. Pectin and pectin-based composite materials: beyond food texture. Molecules. 2018;23(4):942. doi: 10.3390/molecules23040942
62. Sriamornsak P. *Chemistry of pectin and its pharmaceutical uses: a review*. Silpakorn Univ Int J. 2003;3:206–228.
63. Liang W-L, Liao J-S, Qi J-R, et al. Physicochemical characteristics and functional properties of high methoxyl pectin with different degree of esterification. Food Chem. 2022;375:131806. doi: 10.1016/j.foodchem.2021.131806
64. Rouaz K, Chiclana-Rodríguez B, Nardi-Ricart A, et al. Excipients in the paediatric population: a review. Pharmaceutics. 2021;13(3):387. doi: 10.3390/pharmaceutics13030387
65. Commission E. Regulation No 1333/2008 of European parliament and of the council of 16 December 2008 on food additives. 2008 [cited 2024 Jul 17]; Available from: https://eur-lex.europa.eu/LexUriServ/LexUriServ.do?uri=CONSLEG:2008R1333:20120625:EN:PDF
66. Commission, E. Additives database. 2024 [cited 2024 Jul 17]; Available from: https://ec.europa.eu/food/food-feed-portal/screen/food-additives/search
67. Commission, E. Regulation (EC) No 1334/2008 of the european parliament and of the council of 16 December 2008 on flavourings and certain food ingredients with flavouring properties for use in and on foods. 2008 [cited 2024 Jul 17]; Available from: https://eur-lex.europa.eu/legal-content/EN/TXT/PDF/?uri=CELEX:32008R1334
68. Bendicho-Lavilla C, Rodríguez-Pombo L, Januskaite P, et al. *Ensuring the quality of 3D printed medicines: integrating a balance into a pharmaceutical printer for in-line uniformity of mass testing*. J Drug Deliv Sci Technol. 2024;92:105337. doi: 10.1016/j.jddst.2024.105337
69. Bruker. Application report XRD 36. X-Ray powder diffraction (XRPD) in pharma: amorphous content determination and degree of crystallinity. 2017 [cited 2024 Apr 20]; Available from: https://my.bruker.com/acton/attachment/2655/f-0dc2/1/-/-/-/-/45-04%20XRD%20AN%2036%20D8A%20XRPD%20in%20Pharma.pdf?utm_term=PDF%20XRD%20App%20Rpt%2036%20Pharma%20Amorphous&utm_content=landing+page&utm_source=Act-On+Software&utm_medium=landing+page&cm_mmc=Act-On%20Software-_-Landing%20Page-_-_-PDF%20XRD%20App%20Rpt%2036%20Pharma%20Amorphous&sid=TV2:UCBrt5RuS
70. Monsoor MA, Kalapathy U, Proctor A. Determination of polygalacturonic acid content in pectin extracts by diffuse reflectance fourier transform infrared spectroscopy. Food Chem. 2001;74(2):233–238. doi: 10.1016/S0308-8146(01)00100-5
71. Kpodo FM, Agbenorhevi JK, Alba K, et al. Pectin isolation and characterization from six okra genotypes. Food Hydrocoll. 2017;72:323–330.
72. Iñiguez SE, Takiguchi FT. Relación de la clase mólar y la fuerza de la masticación en pacientes de 7 a 10 años de edad. 2019 [cited 2024 Apr 17]; Available from: https://www.odonto.unam.mx/sites/default/files/inline-files/SARA%20EDITH%20I%C3%91IGUEZ%20%20MENDEZ.pdf
73. Gupta A, Chidambaram N, Khan MA. An index for evaluating difficulty of chewing index for chewable tablets. Drug Dev Ind Pharm. 2015;41(2):239–243. doi: 10.3109/03639045.2013.858736
•• **of considerable interest.**
74. Nyamweya NN, Kimani SN, Abuga KO. Chewable antacid tablets: are disintegration tests relevant? AAPS PharmScitech. 2020;21(5):139. doi: 10.1208/s12249-020-01696-y
75. Ahmed KK, Kassab HJ, Al Ramahi IJ, et al. Taste masking of steroids for oral formulations. Turk J Pharm Sci. 2024;20(6):352–360. doi: 10.4274/tjps.galenos.2023.24968
76. Chachlioutaki K, Karavasili C, Mavrokefalou E-E, et al. Quality control evaluation of paediatric chocolate-based dosage forms: 3D printing vs mold-casting method. Int J Pharm. 2022;624:121991. doi: 10.1016/j.ijpharm.2022.121991
77. Europe, E.C.o. 5.17.1. Recommendations on dissolution testing. 2024 [cited 2024 Jan 12]. Available from: https://pheur.edqm.eu/internal/924ea280af2d44feb979d7cdcb106b55/11-5/11-5/page/51701E.pdf
78. PubChem. Hydrocortisone. 2023 [cited 2023 May 4]; Available from: https://pubchem.ncbi.nlm.nih.gov/compound/Hydrocortisone
79. Friciu M, Chefson A, Leclair G. Stability of hydrocortisone, Nifedipine, and nitroglycerine compounded preparations for the treatment of anorectal conditions. Can J Hosp Pharm. 2016;69(4):329–333. doi: 10.4212/cjhp.v69i4.1578
80. Naik RM, Gumpula S, Mhaskar PS. Stability indicating RP-HPLC-DAD method for the simultaneous estimation of hydrocortisone and ketoconazole in tablet dosage form. Int J Pharm Sci Res. 2018;4(1):219–228.
81. Ayyoubi S, van Kampen EEM, Kocabas LI, et al. 3D printed, personalized sustained release cortisol for patients with adrenal insufficiency. Int J Pharm. 2023;630:122466. doi: 10.1016/j.ijpharm.2022.122466
82. FDA. 3D printing medical devices at the point of care: discussion paper. 2021 [cited 2024 May 7]; Available from: https://www.fda.gov/media/154729/download
83. FDA. Distributed manufacturing and point-of-care manufacturing of drugs. 2022 Dec 13 [cited 2023 Nov 7]; Available from: https://www.fda.gov/media/162157/download
84. MHRA. Consultation on point of care manufacturing. 2023 Jan 25 [cited 2023 Apr 3]; Available from: https://www.gov.uk/government/consultations/point-of-care-consultation/consultation-on-point-of-care-manufacturing
85. Commission, E. Conformity assessment procedures for 3D printing and 3D printed products to Be used in a medical context for COVID-19. 2020 [cited 2024 Jul 29]; Available from: https://health.ec.europa.eu/document/download/000cf966-c81e-41d7-a452-1b2d4ce17230_en?filename=md_mdcg_qa_3d_ppp_covid-19_en.pdf
86. EMA. *Guideline on pharmaceutical development of medicines for paediatric use* EMA/CHMP/QWP/805880/2012. The Netherlands: European Medicines Agency; 2012.
87. Europe, C.o. 2.9.3. Dissolution test for solid dosage forms. 2023 [cited 2024 Aug 1]; Available from: https://pheur.edqm.eu/internal/fdbcbed56ac54a699ba8a5405688db95/11-5/11-5/page/20903E.pdf
88. EMA. Guideline on the investigation of bioequivalence. 2010 [cited 2024 Aug 1]; Available from: https://www.ema.europa.eu/en/documents/scientific-guideline/guideline-investigation-bioequivalence-rev1_en.pdf
89. Benet LZ, Broccatelli F, Oprea TI. BDDCS applied to over 900 drugs. Aaps J. 2011;13(4):519–547. doi: 10.1208/s12248-011-9290-9
90. Europe, C.o. 2.6.12. Microbiological examination of non-sterile products: microbial enumeration tests. 2021 [cited 2024 Aug 1];

Available from: https://pheur.edqm.eu/app/11-5/content/11-5/20612E.htm?highlight=on&terms=2.6.12.%20microbiological%20examination&terms=microbiological&terms=2.6.12&terms=examination

91. Europe, C.o. 2.6.13. Microbiological examination of non-sterile products: test for specified micro-organisms. 2021 [cited 2024 Aug 1]; Available from: https://pheur.edqm.eu/app/11-5/content/11-5/20613E.htm?highlight=on&terms=2.6.13.%C2%A0microbiological%20examination%20of%20non-sterile%20products&terms=2.6.13.%20microbiological%20examination%20of%20non-sterile%20products&terms=of&terms=microbiological&terms=2.6.13&terms=sterile&terms=products&terms=of%20products
92. Europe, C.o. 5.1.4. Microbiological quality of non-sterile pharmaceutical preparations and substances for pharmaceutical use. 2021 [cited 2024 Aug 1]; Available from: https://pheur.edqm.eu/app/11-5/content/11-5/50104E.htm?highlight=on&terms=5.1.4.%20microbiological%20quality%20of%20non-sterile%20pharmaceutical%20preparations%20and%20substances%20for%20pharmaceutical%20use&terms=and&terms=of%20microbiological&terms=for&terms=of&terms=quality&terms=substances%20for%20pharmaceutical%20use&terms=for%20microbiological%20quality%20of&terms=use%20and&terms=non-sterile%20preparations&terms=and%20for&terms=non&terms=preparations%20for&terms=use&terms=of%20pharmaceutical%20preparations&terms=of%20non-sterile&terms=for%20non-sterile%20pharmaceutical&terms=5.1.4&terms=of%3A%20%E2%80%93use%20of&terms=use%20of&terms=for%20microbiological%20quality